

Hippocampal transcriptomic responses to cellular dissociation

Rayna M. Harris^{1,2,3}, Hsin-Yi Kao^{3,4,5}, Juan Marcos Alarcón^{3,6,7}, Hans A. Hofmann^{1,3}, André A. Fenton^{3,4,5,6,7}

***For correspondence:**

afenton@nyu.edu (AAF)

† Funding Sources include:
NINDS: NS091830 to JMA
NSF: IOS-1501704 to HAH
NIMH: 5R25MH059472-18
UT Austin Graduate School
Continuing Fellowship to RMH
Helmsley Foundation for
Advanced Training at the
Interface of Biology and
Computational Science to MBL
Helmsley Innovation Award
to AAF and HAH
Grass Foundation to MBL
Michael Vasinkevich to AAF

¹Dept. Integrative Biology; Center for Computational Biology and Bioinformatics, The University of Texas at Austin; ²Dept. of Population Health and Reproduction, University of California, Davis; ³Neural Systems & Behavior Course, Marine Biological Laboratory; ⁴Center for Neural Science, New York University; ⁵Neuroscience Institute at the New York University Langone Medical Center, New York University; ⁶Dept. of Pathology, SUNY Downstate Medical Center; ⁷The Robert F. Furchgott Center for Neural and Behavioral Science, SUNY Downstate Medical Center

Abstract Single-neuron gene expression studies may be especially important for understanding nervous system structure and function because of the neuron-specific functionality and plasticity that defines functional neural circuits. Cellular dissociation is a prerequisite technical manipulation for single-cell and single cell-population studies, but the extent to which the cellular dissociation process affects neural gene expression has not been determined. This information is necessary for interpreting the results of experimental manipulations that affect neural function such as learning and memory. The goal of this research was to determine the impact of chemical cell dissociation on brain transcriptomes. We compared gene expression of microdissected samples from the dentate gyrus (DG), CA3, and CA1 subfields of the mouse hippocampus either prepared by a standard tissue homogenization protocol or subjected to a chemical cellular dissociation procedure. We report that compared to homogenization, chemical cellular dissociation alters about 350 genes or 2% of the hippocampal transcriptome. While only a few genes canonically implicated in long-term potentiation (LTP) and fear memory change expression levels in response to the dissociation procedure, these data indicate that sample preparation can affect gene expression profiles, which might confound interpretation of results depending on the research question. This study is important for the investigation of any complex tissues as research effort moves from subfield level analysis to single cell analysis of gene expression.

Nervous systems are comprised of diverse cell types that express different genes to serve distinct functions. Even within anatomically-defined subfields of the brain, there are identifiable subclasses of neurons that belong to distinct functional circuits (*Danielson et al., 2016; Mizuseki et al., 2011; Namburi et al., 2015*). Cellular diversity is even greater when we consider that specific cells within a functional class can be selectively altered by neural activity in the recent or distant past (*Denny et al., 2014; Garner et al., 2012; Ramirez et al., 2013; Reijmers et al., 2007*). This complexity can confound the interpretation of transcriptome data collected from bulk samples containing hundreds to tens of thousands of cells that represent numerous cellular subclasses at different levels of diversity.

Recent advances in tissue harvesting and sequencing technologies have allowed detailed analyses of genome-scale gene expression profiles at the level of single-cell populations in the context

43 of brain and behavior studies (*Mo et al., 2015; Chalancon et al., 2012; Lacar et al., 2016; Moffitt*
44 *et al., 2018; Nowakowski et al., 2018; Raj et al., 2018*). These approaches have led to systems-level
45 insights into the molecular substrates of neural function and to the discovery and validation of can-
46 didate pathways regulating physiology and behavior. Current methods for dissociating tissues into
47 single-cell suspensions include mechanical and enzymatic treatments (*Jager et al., 2016*). To com-
48 plement the efforts allowing for single-neuron analysis of transcriptional activity, it is necessary to
49 understand the extent to which the dissociation treatment of tissue samples prior to single-cell
50 transcriptome analysis might confound interpretation of the results.

51 Here we aimed to determine if enzymatic dissociation itself alters the transcriptome of the hip-
52 pocampus. We did not compare single-cell RNA-seq data to bulk tissue RNA-seq data because
53 that is orthogonal to the present research question. Instead, we compared tissue level expression
54 of microdissected samples from the dentate gyrus (DG), CA3, and CA1 hippocampal subfields (*Fig-*
55 *ure 1*). Samples were prepared by a standard homogenization protocol and the sequencing results
56 were compared to corresponding samples that were dissociated as if they were being prepared
57 for single-cell sequencing (Fig 1A). We used the Illumina HiSeq platform for sequencing, Kallisto
58 for transcript abundance estimation (*Bray et al., 2016*) and DESeq2 for differential gene expres-
59 sion profiling (*Love et al., 2014*). Data and code are available at NCBI's Gene Expression Omnibus
60 Database (accession number GSE99765), as well as on GitHub ([https://github.com/raynamharris/](https://github.com/raynamharris/DissociationTest)
61 [DissociationTest](#)) with an archived version at the time of publication available on Zenodo (*Harris,*
62 *2019*). A more detailed description of the methods is provided in the supplementary "Detailed
63 Methods" section.

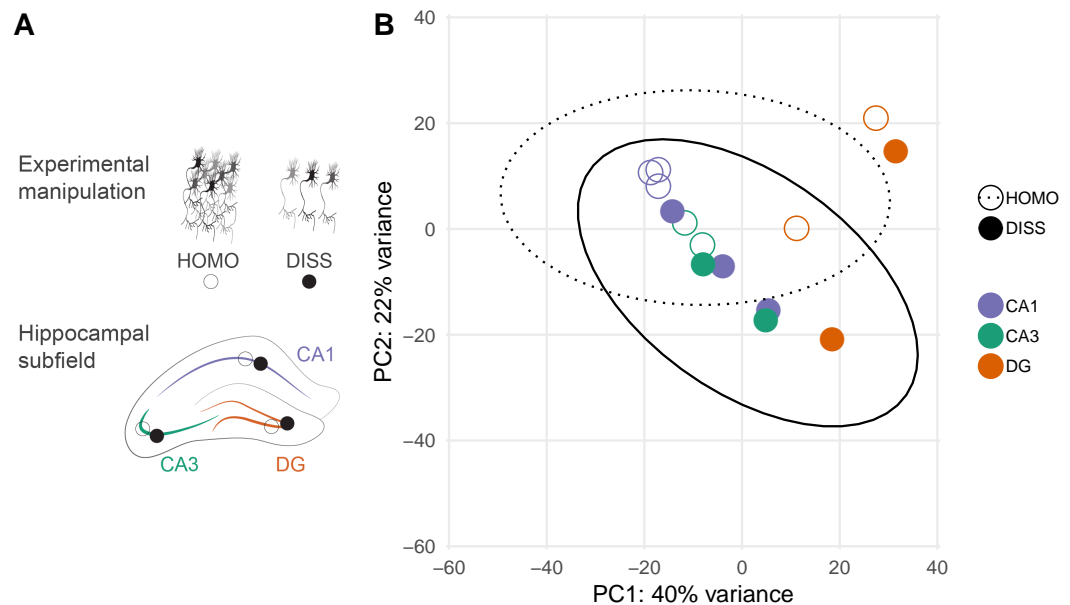


Figure 1. Experimental design and global expression gene expression patterns. A) Experimental design. Two tissue samples were taken from three hippocampal subfields (CA1, CA3, and DG) from 300 μ m brain slices. Two adjacent samples were processed using a homogenization (HOMO) protocol or dissociated (DISS) before processing for tissue level gene expression profiling. **B)** Dissociation does not yield subfield-specific changes in gene expression between homogenized (HOMO, open circles, dotted ellipse) and dissociated tissues (DISS, filled circles, solid ellipse). PC1 accounts for 40% of all gene expression variation and by inspection, separates the DG samples (orange circles) from the CA1 (purple circles) and CA3 samples (green circles). PC2 accounts for 22% of the variation in gene expression and varies significantly with treatment. The ellipses estimate the 95% confidence interval for a multivariate t-distribution for homogenized (dashed line) and dissociated (solid line) samples.

64 Here we analyze transcriptome data from the CA1, CA3, and dentate gyrus (DG) subfields of

Two-way contrast	Increased expression	Decreased expression	% DEGs/Total
CA1 vs DG	222	262	2.90%
CA3 vs DG	45	53	0.50%
CA1 v. CA3	17	1	0.10%
DISS vs HOMO	288	56	2.10%

Table 1. Differentially expressed genes by subfield and treatment. The total number and percent of differentially expressed genes (DEGs) for four two-way contrasts were calculated using DESeq2. Increased expression cutoffs are defined as log fold-change > 0; $p < 0.1$ while decreased expression is defined as log fold-change < 0; $p < 0.1$. % DEGs/Total: The sum of up and down regulated genes divided by the total number of genes analyzed (16,709) multiplied by 100%. This table shows that differences between dissociated (DISS) tissue and homogenized (HOMO) tissues are on the same scale as those between the CA1 and DG subfields of the hippocampus.

65 the hippocampus subjected to one of two treatments (homogenize (HOMO) or dissociated (DISS)
66 (**Figure 1**). The null hypothesis is that treatment effects will not be different between hippocam-
67 pal subfields. However it is known, that there are subfield expression differences (**Cembrowski**
68 **et al., 2016a,b, 2018; Hawrylycz et al., 2012; Lein et al., 2004**). DNA microarray followed by in
69 situ hybridization was used to validate region-specific expression patterns of 100 differentially ex-
70 pressed genes (**Lein et al., 2004**). Hierarchical clustering was used to visualize the top 30 differ-
71 entially expressed genes ($p < 0.01$) across hippocampal subfields (**Hawrylycz et al., 2012**). RNA-
72 seq experiments on spatially distinct hippocampal subfield samples gave good agreement with
73 immunohistochemical (IHC) data, correctly predicting the enriched populations in 81% of cases
74 (124/153 genes) where coronal IHC images were available (**Cembrowski et al., 2016a**). Because
75 the CA1 region is more vulnerable to anoxia than other hippocampus cell regions (**Pulsinelli et al.,**
76 **1982**), region-specific differences in the influence of treatment type might also be expected.

77 We first quantified the effects of treatment and hippocampus subfield on differential gene ex-
78 pression using principal component dimensionality reduction. Samples with similar expression
79 patterns will cluster in the space defined by principal component dimensions. If there are large dif-
80 ferences in expression according to treatment, the samples will separate into two non-overlapping
81 clusters. Principal component analysis (PCA) suggests that dissociation does not have a large ef-
82 fect on gene expression because the samples do not form distinct, non-overlapping clusters of
83 homogenized and dissociated samples (**Figure 1B**). In this analysis the first principal component
84 (PC1) accounts for 40% of the variance and distinguishes DG samples from the CA1 and CA3 sam-
85 ples. A two-way treatment-by-region ANOVA confirmed a significant effect of region ($F_{2,11} = 17.69$;
86 $p = 0.0004$). Post hoc Tukey tests confirmed $CA1 = CA3 < DG$. The second principal component
87 (PC2) accounts for 22% of the variation in gene expression and varies significantly with treatment
88 ($F_{1,12} = 6.13$; $p = 0.03$). None of the higher principal components showed significant variation ac-
89 cording to either subfield or treatment. Thus enzymatic dissociation causes differential gene ex-
90 pression but a fraction of what is due to subregion specificity.

91 Next, we identified the 344 differentially expressed genes between homogenized and disso-
92 ciated tissues, accounting for 2.1% of the 16,709 measured genes (**Table 1** and **Table 2**). Most
93 differentially expressed genes showed increased expression (288 genes) rather than decreased
94 expression (56 genes) in response to dissociation (**Figure 2A**). We found that 2.9% of the transcrip-
95 tome is differentially expressed between CA1 and DG, with a roughly symmetric distribution of
96 differential gene expression (not shown). A heatmap of the top 30 differentially expressed genes
97 illustrates the fold-change differences across samples (**Figure 2B**). Enzymatic dissociation appears
98 to activate gene expression, suggesting the process overall, induces rather than suppresses a cel-
99 lular response.

100 Because the hippocampus is central to learning and memory, we asked whether the expres-
101 sion of genes and pathways known to be involved in learning and memory is affected by disso-

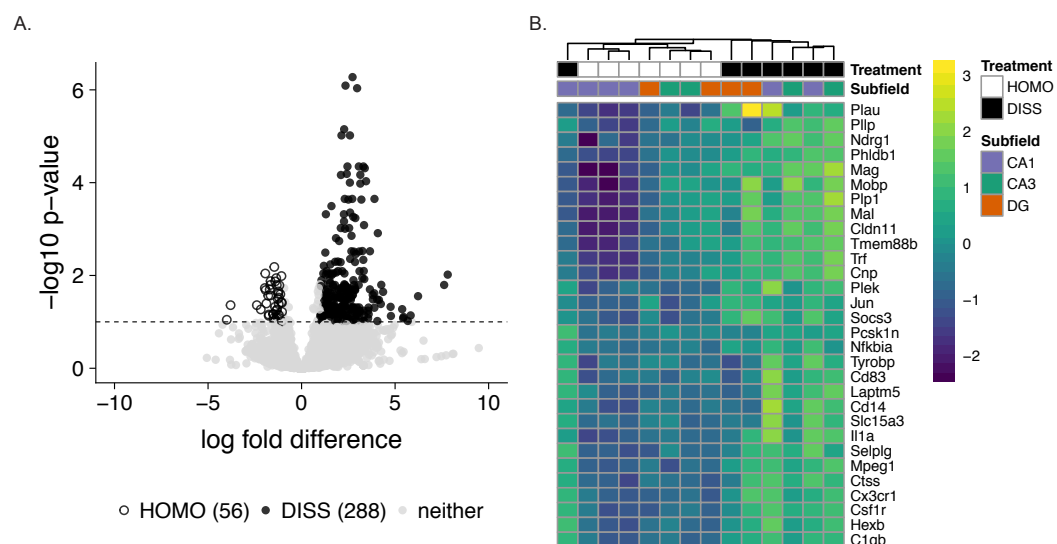


Figure 2. Enzymatic dissociation has a moderate effect on hippocampal gene expression patterns compared to homogenized tissue. **A)** Volcano plot showing gene expression fold-difference and significance between treatment groups. We found that 56 genes are up-regulated in the homogenization control group (open circles) while 288 genes are up-regulated in the dissociated treatment group (filled dark grey circles). Genes below the $p\text{-value} < 0.1$ (or $-\log p\text{-value} < 1$) are shown in light grey. **B)** Heatmap showing the top 30 differentially expressed genes between dissociated and homogenized tissue. Square boxes at the top are color coded by sample (white: homogenized, grey: dissociated, purple: CA1, green: CA3, orange: DG). Within the heatmap, log fold difference levels of expression are indicated by the blue-green-yellow gradient with lighter colors indicating increased expression.

102 ciation. We first examined expression of 240 genes that have been implicated in long-term po-
 103 tentiation (LTP) (*Sanes and Lichtman, 1999*) **Table 2** and found that the expression of only nine of
 104 these genes was altered by enzymatic dissociation treatment. The expression of *CACNA1E*, *GABRB1*,
 105 *GRIN2A* was downregulated in response to dissociation treatment (meaning that their activity could
 106 be underestimated in an experiment using enzymatic treatment to dissociate tissue) while *IL1B*,
 107 *ITGA5*, *ITGAM*, *ITGB4*, *ITGB5*, and *MAPK3* were upregulated in response to dissociation. *CACNA1E* is
 108 a subunit of L-type calcium channels, which are necessary for LTP induction of mossy fiber input
 109 to CA3 pyramidal neurons (*Kapur et al., 1998*). *GABRB1* encodes the Gamma-Aminobutyric Acid
 110 (GABA) A Receptor Beta subunit, and *GRIN2A* encodes the Glutamate Ionotropic Receptor NMDA
 111 Type 2A subunit. Because GABA receptors and NMDA receptors mediate inhibitory and excitatory
 112 neurotransmission in hippocampus, respectively, enzymatic dissociation could itself alter accurate
 113 estimation of the roles of these receptors. *IL1B* encodes interleukin-1beta, a cytokine that plays a
 114 key role in the immune response to infection and injury but is also critical for maintaining LTP in
 115 healthy brains (*Schneider et al., 1998*). The integrin class of cell adhesion molecules plays an im-
 116 portant role in synaptic plasticity, particularly in stabilization and consolidation of LTP (*Bahr et al.,*
 117 *1997; McGeachie et al., 2011*). Overall, our analysis demonstrates that the expression of only a few
 118 canonical LTP-related genes is affected by the tissue preparation method.

119 More recently, RNA sequencing was used in combination with ribosomal profiling to quantify
 120 the translational status and transcript levels in the mouse hippocampus after contextual fear condi-
 121 tioning (*Cho et al., 2015*). The analysis revealed that memory formation was regulated by learning-
 122 induced suppression of ribosomal protein-coding genes and suppression of a subset of genes
 123 via inhibition of estrogen receptor 1 signaling in the hippocampus. We cross-referenced learning-
 124 induced differential gene expression from (*Cho et al., 2015*), to identify genes that are altered by
 125 both fear-conditioning and enzymatic dissociation. We found that *BTG2*, *FOSB*, *FN1*, *IER2*, and *JUNB*
 126 were all upregulated in response to enzymatic dissociation and fear-conditioning while *Enpp2* was
 127 upregulated in response to dissociation but down-regulated in fear-conditioning via estrogen re-

128 ceptor 1 inhibition. *BTG2* is required for proliferation and differentiation of neurons during adult
129 hippocampal neurogenesis and may be involved in the formation of contextual memories *Farioli-*
130 *Vecchioli et al. (2009)*. FOSB and JUNB are dimers that form the transcription factor complex AP-1
131 that is often used as a marker for neural activity (*Alberini, 2009*). *IER2* is also a transcription factor
132 that, along with FOS and JUN, as well as *FN1*, which encodes the adhesion molecule Fibronectin,
133 was not included in the (*Sanes and Lichtman, 1999*) list as important for LTP but was differentially
134 expressed following fear-conditioning in (*Cho et al., 2015*). These comparisons show that tissue
135 preparation methods can alter expression in a small subset of genes that may be important for
136 LTP.

137 This study was motivated by the possibility of single cell sequencing, although we did not con-
138 duct single-neuron sequencing in this study. A single-cell study would not have made it possible
139 to test our hypothesis of how the process of cellular dissociation affects gene expression relative
140 to tissue homogenization, because the RNA from single cells can't be recovered after tissue ho-
141 mogenization. To compare single cell transcriptomes that are obtained without dissociation, we
142 could have used mechanical dissociation for example by laser microdissection and capture or by
143 microaspiration but this was not deemed practical because these are substantially more difficult,
144 expensive, and low-throughput procedures compared to enzymatic dissociation of cells. Given the
145 present findings that enzymatic dissociation may itself induce gene expression, it may be useful
146 to first prepare tissues with transcription and translation blockers like puromycin and actinomycin
147 to arrest gene expression activity before cellular dissociation (*Flexner et al., 1963; Solntseva and*
148 *Nikitin, 2012*), but potential additional effects of these treatments will also need to be investigated
149 and controlled using appropriate experimental designs.

150 We set out to identify the extent to which the process of chemical cellular dissociation, affects
151 neural gene expression profiles, because the process necessarily precedes high-throughput single
152 cell analysis of complex tissues. We found that gene expression in hippocampal subfields is
153 changed by tissue preparation procedures (cellular dissociation versus homogenization) and cross-
154 referenced the differentially expressed genes with genes and pathways known to be involved in
155 hippocampal LTP, learning and memory. While it is encouraging that the activity of only a small
156 number of genes and pathways involved in LTP, learning and memory appears affected by dissocia-
157 tion, it is also important to effectively use experimental design to control for technical artifacts. The
158 present findings provide insight into how cellular manipulations influence gene expression, which
159 is important because it is increasingly necessary to dissociate cells in tissue samples for single cell
160 or single cell-type studies.

161 **Acknowledgments**

162 We thank members of the Hofmann and Fenton Labs, Boris Zemelman, Laura Colgin, and Misha
163 Matz for helpful discussions. We thank Dennis Wylie for insightful comments on earlier versions
164 of this manuscript. We thank the GSAF for library preparation and sequencing. The bioinformatic
165 workflow was inspired heavily by Center for Computational Biology's Bioinformatics Curriculum
166 and Software Carpentry Curriculum on the Unix Shell, Git for Version Control, and R for Repro-
167 ducible Research. This work is supported by a Society for Integrative Biology (SICB) Grant in Aid
168 of Research (GIAR) grant and a UT Austin Graduate School Continuing Fellowship to RMH; a gen-
169 erous gift from Michael Vasinkevich to AAF; NIH-NS091830 to JMA, IOS-1501704 to HAH; NIMH-
170 5R25MH059472-18. The authors declare no competing interests.

171 **Detailed methods**

172 All animal care and use comply with the Public Health Service Policy on Humane Care and Use of
173 Laboratory Animals and were approved by the New York University Animal Welfare Committee. A 1-
174 year-old female C57BL/6J mouse was taken from its cage, anesthetized with 2% (vol/vol) isoflurane
175 for 2 minutes and decapitated. Transverse 300 μm brain slices were cut using a vibratome (model

176 VT1000 S, Leica Biosystems, Buffalo Grove, IL) and incubated at 36°C for 30 min and then at room
177 temperature for 90 min in oxygenated artificial cerebrospinal fluid (aCSF in mM: 125 NaCl, 2.5
178 KCl, 1 MgSO₄, 2 CaCl₂, 25 NaHCO₃, 1.25 NaH₂PO₄ and 25 Glucose) as in Pavlowsky and Alarcon,
179 2012. Tissue adjacent samples were collected from CA1, CA3, and DG, respectively in the dorsal
180 hippocampus by punch (0.25 mm, P/N: 57391; Electron Microscopy Sciences, Hatfield, PA) (Fig 1A).

181 The homogenized (HOMO) samples were processed using the manufacturer instructors for the
182 Maxwell 16 LEV RNA Isolation Kit (Promega, Madison, WI). The dissociated (DISS) samples were
183 incubated for 75 minutes in aCSF containing 1 mg/ml pronase at room temperature, then vortexed
184 and centrifuged. The incubation was terminated by replacing aCSF containing pronase with aCSF.
185 The sample was then vortexed, centrifuged, and gently triturated by 200- μ l pipette tip twenty times
186 in aCSF containing 1% FBS. The sample was centrifuged and used as input for RNA isolation using
187 the Maxwell 16 LEV RNA Isolation Kit (Promega, Madison, WI).

188 RNA libraries were prepared by the Genomic Sequencing and Analysis Facility at the University
189 of Texas at Austin using the Illumina HiSeq platform. Raw reads were processed and analyzed
190 on the Stampede Cluster at the Texas Advanced Computing Facility (TACC). Samples yielded an
191 average of 4.9 +/- 2.6 million reads. Quality of the data was checked using the program FASTQC.
192 Low quality reads and adapter sequences were removed using the program Cutadapt (*Martin,*
193 *2011*). We used Kallisto for read pseudoalignment to the Gencode M11 mouse transcriptome and
194 for transcript counting (*Bray et al., 2016; Mudge and Harrow, 2015*). On average, 61.2% +/- 20.8%
195 of the trimmed reads were pseudoaligned to the mouse transcriptome.

196 Kallisto transcript counts were imported into R (*R Development Core Team, 2013*) and aggre-
197 gated to yield gene counts using the 'gene' identifier from the Gencode reference transcriptome.
198 We used DESeq2 for gene expression normalization and quantification of gene level counts (*Love*
199 *et al., 2014*). We used a threshold of a false discovery corrected (FDR) p-value < 0.1. Statistics on
200 the principal component analysis (PCA) were conducted in R. The hierarchical clustering analysis
201 was conducted and visualized using the R package pheatmap (*Kolde, 2015*) with the RColorBrewer
202 R packages for color modifications (*Neuwirth, 2014*). PCA was conducted in R using the DESeq2
203 and genefilter R packages (*Gentleman R et al., 2017; Love et al., 2014*) and visualized using the
204 ggplot2 and cowplot R packages (*Wilke, 2016; Wickham, 2009*).

205 The raw sequence data and intermediate data files are archived in NCBI's Gene Expression
206 Omnibus Database (accession numbers GSE99765). The data and code are available on GitHub
207 (<https://github.com/raynamharris/DissociationTest>), with an archived version at the time of publica-
208 tion available at Zenodo (Harris et al., 2017). A Jupyter notebook containing a cloud-based, open-
209 access analysis of GEO dataset GSE99765 (<https://www.ncbi.nlm.nih.gov/gds/?term=GSE99765>) cre-
210 ated using BioJupies (*Torre et al., 2018*) is available at <http://amp.pharm.mssm.edu/biojupies/notebook/zySloEXuZ>.

212 References

- 213 **Alberini CM.** Transcription factors in long-term memory and synaptic plasticity. *Physiological Reviews.* 2009
214 1; 89(1):121–45. <http://www.ncbi.nlm.nih.gov/pubmed/19126756>, doi: 10.1152/physrev.00017.2008.
- 215 **Bahr BA,** Staubli U, Xiao P, Chun D, Ji ZX, Esteban ET, et al. Arg-Gly-Asp-Ser-selective adhesion and the stabiliza-
216 tion of long-term potentiation: pharmacological studies and the characterization of a candidate matrix recep-
217 tor. *The Journal of neuroscience : the official journal of the Society for Neuroscience.* 1997 2; 17(4):1320–9.
218 <http://www.ncbi.nlm.nih.gov/pubmed/9006975>.
- 219 **Bray NL,** Pimentel H, Melsted P, Pachter L. Near-optimal probabilistic RNA-seq quantification. *Nature Biotech-*
220 *nology.* 2016 4; 34(5):525–527. <http://www.nature.com/doi/10.1038/nbt.3519>, doi: 10.1038/nbt.3519.
- 221 **Cembrowski MS,** Bachman JL, Wang L, Sugino K, Shields BC, Spruston N. Spatial Gene-Expression Gradients
222 Underlie Prominent Heterogeneity of CA1 Pyramidal Neurons. *Neuron.* 2016 1; 89(2):351–368. [http://www.](http://www.ncbi.nlm.nih.gov/pubmed/26777276)
223 [ncbi.nlm.nih.gov/pubmed/26777276](http://www.ncbi.nlm.nih.gov/pubmed/26777276), doi: 10.1016/j.neuron.2015.12.013.
- 224 **Cembrowski MS,** Wang L, Lemire AL, Copeland M, DiLisio SF, Clements J, et al. The subiculum is a patchwork
225 of discrete subregions. *eLife.* 2018 10; 7. <https://elifesciences.org/articles/37701>, doi: 10.7554/eLife.37701.

- 226 **Cembrowski MS**, Wang L, Sugino K, Shields BC, Spruston N. Hipposeq: A comprehensive RNA-seq database of
227 gene expression in hippocampal principal neurons. *eLife*. 2016 4; 5(APRIL2016):e14997. <http://elifesciences.org/lookup/doi/10.7554/eLife.14997>, doi: 10.7554/eLife.14997.
- 229 **Chalancon G**, Ravarani CNJ, Balaji S, Martinez-Arias A, Aravind L, Jothi R, et al. Interplay between gene ex-
230 pression noise and regulatory network architecture. *Trends in Genetics*. 2012 5; 28(5):221–232. <http://www.ncbi.nlm.nih.gov/pubmed/22365642>, doi: 10.1016/j.tig.2012.01.006.
- 232 **Cho J**, Yu NK, Choi JH, Sim SE, Kang SJ, Kwak C, et al. Multiple repressive mechanisms in the hippocampus during
233 memory formation. *Science (New York, NY)*. 2015 10; 350(6256):82–7. <http://www.ncbi.nlm.nih.gov/pubmed/26430118>, doi: 10.1126/science.aac7368.
- 235 **Danielson NB**, Zaremba JD, Kaifosh P, Bowler J, Ladow M, Losonczy A. Sublayer-Specific Coding Dynamics
236 during Spatial Navigation and Learning in Hippocampal Area CA1. *Neuron*. 2016 8; 91(3):652–665. <http://linkinghub.elsevier.com/retrieve/pii/S0896627316302987>, doi: 10.1016/j.neuron.2016.06.020.
- 238 **Denny CA**, Kheirbek MA, Alba EL, Tanaka KF, Brachman RA, Laughman KB, et al. Hippocampal
239 memory traces are differentially modulated by experience, time, and adult neurogenesis. *Neu-
240 ron*. 2014 7; 83(1):189–201. <http://www.pubmedcentral.nih.gov/articlerender.fcgi?artid=4169172&tool=pmcentrez&rendertype=abstract>, doi: 10.1016/j.neuron.2014.05.018.
- 242 **Farioli-Vecchioli S**, Saraulli D, Costanzi M, Leonardi L, Cinà I, Micheli L, et al. Impaired terminal differentiation
243 of hippocampal granule neurons and defective contextual memory in PC3/Tis21 knockout mice. *PLoS one*.
244 2009 12; 4(12):e8339. <http://www.ncbi.nlm.nih.gov/pubmed/20020054>, doi: 10.1371/journal.pone.0008339.
- 245 **Flexner JB**, Flexner LB, Stellar E. Memory in Mice as Affected by Intracerebral Puromycin. *Science*.
246 1963; 141(3575):57–59. <http://www.sciencemag.org/cgi/doi/10.1126/science.141.3575.57>, doi: 10.1126/sci-
247 ence.141.3575.57.
- 248 **Garner AR**, Rowland DC, Hwang SY, Baumgaertel K, Roth BL, Kentros C, et al. Generation of a synthetic memory
249 trace. *Science*. 2012 3; 335(6075):1513–6. <http://www.sciencemag.org/content/335/6075/1513.abstract>, doi:
250 10.1126/science.1214985.
- 251 **Gentleman R HW Carey V**, F H, Gentleman R, Carey V, Huber W, Hahne F, genefilter: genefilter: methods for
252 filtering genes from high-throughput experiments; 2017.
- 253 **Harris RM**. raynamharris/DissociationTest: GitHub repository for hippocampal transcriptomic responses
254 to cellular dissociation. . 2019 1; <https://zenodo.org/record/2537267#.XDew089Kgn1>, doi: 10.5281/ZEN-
255 ODO.2537267.
- 256 **Hawrylycz MJ**, Lein ES, Guillozet-Bongaarts AL, Shen EH, Ng L, Miller JA, et al. An anatomically comprehensive
257 atlas of the adult human brain transcriptome. *Nature*. 2012 9; 489(7416):391–399. [https://www.nature.com/](https://www.nature.com/articles/nature11405)
258 [articles/nature11405](https://www.nature.com/articles/nature11405), doi: 10.1038/nature11405.
- 259 **Jager LD**, Canda CMA, Hall CA, Heilingoetter CL, Huynh J, Kwok SS, et al. Effect of enzymatic and me-
260chanical methods of dissociation on neural progenitor cells derived from induced pluripotent stem cells.
261 *Advances in medical sciences*. 2016 3; 61(1):78–84. <http://www.ncbi.nlm.nih.gov/pubmed/26523795>, doi:
262 10.1016/j.advms.2015.09.005.
- 263 **Kapur A**, Yeckel MF, Gray R, Johnston D. L-Type Calcium Channels Are Required for One Form of Hippocam-
264 pal Mossy Fiber LTP. *Journal of Neurophysiology*. 1998 4; 79(4):2181–2190. [http://www.ncbi.nlm.nih.gov/](http://www.ncbi.nlm.nih.gov/pubmed/9535977)
265 [pubmed/9535977](http://www.ncbi.nlm.nih.gov/pubmed/9535977), doi: 10.1152/jn.1998.79.4.2181.
- 266 **Kolde R**, pheatmap: Pretty Heatmaps; 2015.
- 267 **Lacar B**, Linker SB, Jaeger BN, Krishnaswami S, Barron J, Kelder M, et al. Nuclear RNA-seq of single neurons
268 reveals molecular signatures of activation. *Nature Communications*. 2016 4; 7:11022. [http://www.ncbi.nlm.](http://www.ncbi.nlm.nih.gov/pubmed/27090946)
269 [nih.gov/pubmed/27090946](http://www.ncbi.nlm.nih.gov/pubmed/27090946), doi: 10.1038/ncomms11022.
- 270 **Lein ES**, Zhao X, Gage FH. Defining a molecular atlas of the hippocampus using DNA microarrays and high-
271 throughput in situ hybridization. *Journal of Neuroscience*. 2004 4; 24(15):3879–89. [http://www.jneurosci.org/](http://www.jneurosci.org/content/24/15/3879)
272 [content/24/15/3879](http://www.jneurosci.org/content/24/15/3879), doi: 10.1523/JNEUROSCI.4710-03.2004.
- 273 **Love MI**, Huber W, Anders S. Moderated estimation of fold change and dispersion for RNA-seq data
274 with DESeq2. *Genome Biology*. 2014 12; 15(12):550. <http://genomebiology.com/2014/15/12/550>, doi:
275 10.1186/s13059-014-0550-8.

- 276 **Martin M.** Cutadapt removes adapter sequences from high-throughput sequencing reads. *EMBnetjournal*.
277 2011; 17(1):10–12.
- 278 **McGeachie AB**, Cingolani LA, Goda Y. Stabilising influence: integrins in regulation of synaptic plasticity.
279 *Neuroscience research*. 2011 5; 70(1):24–9. <https://www.ncbi.nlm.nih.gov/pmc/articles/PMC3242036/>, doi:
280 [10.1016/j.neures.2011.02.006](https://doi.org/10.1016/j.neures.2011.02.006).
- 281 **Mizuseki K**, Diba K, Pastalkova E, Buzsáki G. Hippocampal CA1 pyramidal cells form functionally distinct sub-
282 layers. *Nature Neuroscience*. 2011 8; 14(9):1174–1181. <http://www.ncbi.nlm.nih.gov/pubmed/21822270>, doi:
283 [10.1038/nn.2894](https://doi.org/10.1038/nn.2894).
- 284 **Mo A**, Mukamel E, Davis F, Luo C, Henry G, Picard S, et al. Epigenomic Signatures of Neuronal Diversity in the
285 Mammalian Brain. *Neuron*. 2015 6; 86(6):1369–1384. <http://www.ncbi.nlm.nih.gov/pubmed/26087164>, doi:
286 [10.1016/j.neuron.2015.05.018](https://doi.org/10.1016/j.neuron.2015.05.018).
- 287 **Moffitt JR**, Bambah-Mukku D, Eichhorn SW, Vaughn E, Shekhar K, Perez JD, et al. Molecular, spatial, and
288 functional single-cell profiling of the hypothalamic preoptic region. *Science*. 2018 11; 362(6416):eaau5324.
289 <http://www.ncbi.nlm.nih.gov/pubmed/30385464>, doi: [10.1126/science.aau5324](https://doi.org/10.1126/science.aau5324).
- 290 **Mudge JM**, Harrow J. Creating reference gene annotation for the mouse C57BL6/J genome assembly.
291 *Mammalian Genome*. 2015 10; 26(9-10):366–378. <http://link.springer.com/10.1007/s00335-015-9583-x>, doi:
292 [10.1007/s00335-015-9583-x](https://doi.org/10.1007/s00335-015-9583-x).
- 293 **Namburi P**, Al-Hasani R, Calhoon GG, Bruchas MR, Tye KM. Architectural Representa-
294 tion of Valence in the Limbic System. . 2015; [https://tyelab.mit.edu/wp-content/uploads/](https://tyelab.mit.edu/wp-content/uploads/2016-architectural-representation-of-valence-in-the-limbic-system.pdf)
295 [2016-architectural-representation-of-valence-in-the-limbic-system.pdf](https://tyelab.mit.edu/wp-content/uploads/2016-architectural-representation-of-valence-in-the-limbic-system.pdf), doi: [10.1038/npp.2015.358](https://doi.org/10.1038/npp.2015.358).
- 296 **Neuwirth E**, RColorBrewer: ColorBrewer Palettes; 2014.
- 297 **Nowakowski TJ**, Rani N, Golkaram M, Zhou HR, Alvarado B, Huch K, et al. Regulation of cell-type-specific
298 transcriptomes by microRNA networks during human brain development. *Nature Neuroscience*. 2018 12;
299 21(12):1784–1792. <http://www.ncbi.nlm.nih.gov/pubmed/30455455>, doi: [10.1038/s41593-018-0265-3](https://doi.org/10.1038/s41593-018-0265-3).
- 300 **Pulsinelli Wa**, Brierley JB, Plum F. Temporal profile of neuronal damage in a model of transient forebrain
301 ischemia. *Annals of neurology*. 1982; doi: [10.1002/ana.410110509](https://doi.org/10.1002/ana.410110509).
- 302 **R Development Core Team**, R: a language and environment for statistical computing | GBIF.ORG. Vienna,
303 Austria: R Foundation for Statistical Computing; 2013. <http://www.r-project.org/>.
- 304 **Raj B**, Wagner DE, McKenna A, Pandey S, Klein AM, Shendure J, et al. Simultaneous single-cell profiling of
305 lineages and cell types in the vertebrate brain. *Nature Biotechnology*. 2018 3; 36(5):442–450. [http://www.
306 \[ncbi.nlm.nih.gov/pubmed/29608178\]\(http://www.ncbi.nlm.nih.gov/pubmed/29608178\), doi: \[10.1038/nbt.4103\]\(https://doi.org/10.1038/nbt.4103\).](http://www.ncbi.nlm.nih.gov/pubmed/29608178)
- 307 **Ramirez S**, Liu X, Lin PA, Suh J, Pignatelli M, Redondo RL, et al. Creating a false memory in the hippocampus.
308 *Science*. 2013; doi: [10.1126/science.1239073](https://doi.org/10.1126/science.1239073).
- 309 **Reijmers LG**, Perkins BL, Matsuo N, Mayford M. Localization of a stable neural correlate of associative mem-
310 ory. *Science*. 2007 8; 317(5842):1230–3. <http://www.sciencemag.org/content/317/5842/1230.abstract>, doi:
311 [10.1126/science.1143839](https://doi.org/10.1126/science.1143839).
- 312 **Sanes JR**, Lichtman JW. Can molecules explain long-term potentiation? *Nature neuroscience*. 1999 7; 2(7):597–
313 604. <http://www.ncbi.nlm.nih.gov/pubmed/10404178>, doi: [10.1038/10154](https://doi.org/10.1038/10154).
- 314 **Schneider H**, Pitossi F, Balschun D, Wagner A, del Rey A, Besedovsky HO. A neuromodulatory role of interleukin-
315 1beta in the hippocampus. *Proceedings of the National Academy of Sciences of the United States of America*.
316 1998 6; 95(13):7778–83. <http://www.ncbi.nlm.nih.gov/pubmed/9636227>.
- 317 **Solntseva S**, Nikitin V. Conditioned food aversion reconsolidation in snails is impaired by translation inhibitors
318 but not by transcription inhibitors. *Brain Research*. 2012; 1467:42–47. doi: [10.1016/j.brainres.2012.05.051](https://doi.org/10.1016/j.brainres.2012.05.051).
- 319 **Torre D**, Lachmann A, Ma'ayan A. BioJupies: Automated Generation of Interactive Notebooks for RNA-Seq Data
320 Analysis in the Cloud. *Cell systems*. 2018 11; 7(5):556–561. <http://www.ncbi.nlm.nih.gov/pubmed/30447998>,
321 doi: [10.1016/j.cels.2018.10.007](https://doi.org/10.1016/j.cels.2018.10.007).
- 322 **Wickham H**. ggplot2: Elegant Graphics for Data Analysis. Springer-Verlag New York; 2009. <http://ggplot2.org>,
323 doi: [10.1007/978-0-387-98141-3](https://doi.org/10.1007/978-0-387-98141-3).
- 324 **Wilke CO**, cowplot: Streamlined Plot Theme and Plot Annotations for 'ggplot2'; 2016.

325 **Supplementary Materials**

gene	lfc	padj	direction
Trf	2.72	5.31E-07	DISS
Hexb	2.35	8.10E-07	DISS
Selp1g	2.97	9.22E-07	DISS
C1qb	2.28	7.07E-06	DISS
Csf1r	2.13	9.58E-06	DISS
Ctss	2.59	9.58E-06	DISS
Cnp	2.45	4.48E-05	DISS
Il1a	3.06	4.48E-05	DISS
Mag	3.31	4.48E-05	DISS
Cd14	3.38	4.88E-05	DISS

Table 2. Expression level and fold change of significant genes ($p < 0.1$) between dissociated tissue and homogenized tissue. This table shows the log fold change (lfc), p-value (padj), and direction of upregulation for each gene analyzed. *This is a preview. The full table is available at <https://github.com/raynamharris/DissociationTest/blob/master/results/dissociationDEGs.csv>.*

Sanes & Lichtman Molecules	Related Transcripts
GLUTAMATE RECEPTORS	
GluR1; GluR2	Gria1; Gria2
mGluR1; mGluR4; mGluR5; mGluR7	Grm1; Grm4; Grm5; Grm7
NMDA NR2A; NMDA NR2D; NMDA NR1	Grin1; Grin2a; Grin2d
OTHER NEUROTRANSMITTERS	
norepinephrine and b-adrenergic receptors	Adrb1; Adrb2; Adrb3
adenosine and adenosine 2A receptors	Adra1a; Adra1b; Adra1d; Adra2a
dopamine and D1 dopamine receptors	Th; Drd1
mu and delta opioid receptors	Oprm1; Oprd1
acetylcholine receptors	Chrna1; Chrna7; Chrna3; Chrb1

Table 3. Molecules implicated in hippocampal LTP from Sanes and Lichtman 1999. This table list the molecules review by Sanes and Lichtman in their 1999 review article and the related transcripts that were investigated in this study. *This is a preview. The full table is available at <https://github.com/raynamharris/DissociationTest/blob/master/data/SanesLichtman.csv>*